https://doi.org/10.56295/1ACEG26

THE BOGONG LANDSLIDE, A CASE STUDY INTO AN AUSTRALIAN LANDSLIDE IN UNSATURATED SOILS

Darren Paul, Simon Harbig, Emma O'Brien, Alana Dubowik
WSP, Melbourne, Victoria

ABSTRACT

Over the course of two weeks between 28 September and 12 October 2022 a landslide estimated to have mobilised a volume of 30,000 m^3 of soil occurred on north-facing slopes near Bogong Village in Victoria. Debris arising from the landslide blocked Bogong High Plains Road – the main road to one of Australia's largest ski resorts, Falls Creek, and forced the evacuation of Bogong Village downslope of the landslide. The road needed to be re-opened before May 2023 to allow access to the resort for the 2023 ski season, it being the only road to the resort. Understanding the processes that caused the landslide became critical to informing the design and safe execution of interim works to re-open Bogong High Plains Road. Various lines of evidence including video of the landslide occurring, geomorphological evidence, investigations and analysis informed the development of an engineering geological model for the landslide. The model indicated anomalously deep extremely weathered micaceous granodiorite with a high void ratio at the sheared contact between two plutons. Perhaps owing to their northerly aspect and high evapotranspiration, the soils comprising these slopes preserve high soil suctions. A loss of soil suction arising from wetting fronts that developed over the course of three successive La Niña years was assessed to have triggered the landslide. On the basis of this model, interim works were designed to safely remove a sufficient volume of soils to re-open a single lane of the road. Following the interim works, permanent landslide mitigation was provided, the basis of which was to promote the preservation of soil suctions whilst preserving the natural landscape adjacent to Alpine National Park as far as practical. Understanding the response of the unsaturated soils to prolonged rainfall was critical to informing the design of interim and permanent landslide mitigations. This paper describes the development of the engineering geological model for the Bogong landslide and how the model then informed interim and permanent works to reopen the road and to prevent further landslides.

1 INTRODUCTION AND BACKGROUND

The Bogong landslide occurred upslope of Bogong High Plains Road and Bogong Village as indicated in Figure 1.

Figure 1: Aerial photograph of the Bogong landslide taken 11 November 2022

The cut road batter at the site of the landslide had exhibited signs of instability in the past, including in 2017 at which time the road batter was cut back and benched, with an overall slope angle of about 60° and height of about 15 m (Figure 2). The Bogong landslide of October 2022 was preceded by three years of above average rainfall induced by La Niña climate conditions. Approximately two weeks before the landslide, tension cracks were observed on a track about 90 m back from the roadway (Figure 3). Ongoing movement was observed before the landslide, which ultimately displaced approximately 30,000 m^3 of soil. Spoil and vegetation were deposited across both lanes of the road, completely blocking access between the major towns of Mount Beauty and Falls Creek and threatening Bogong Village downslope of the landslide (Figure 1). Falls Creek is an alpine resort reliant on income from tourism, particularly in winter, making the financial consequences of not opening the road before the 2023 ski season significant and demanding a rapid response.

Figure 2: Left: Road Batter in May 2017 at completion of excavation. Right: Road Batter on 8 October 2022 following landslide initiation

Figure 3: Left: Cracking observed on Spring Saddle Track, 28 September 2022. Right: Cracking observed in face of batter, 5 October 2022

The immediate response involved making the site safe and constructing a bypass road around the landslide. However, the bypass road was steep, unsealed and suitable only for four-wheel drive access. Bogong Village at the base of the landslide was evacuated and, subsequent to that, the works began to clear debris from the top of the landslide working down and clearing material that could safely be removed from the toe of the landslide using remote controlled equipment.

However, a robust interim solution was needed to provide access during the upcoming 2023 ski season and then an ongoing permanent solution required beyond that. Development of that solution required a thorough understanding of what caused the landslide and if the landslide mechanisms could act in the future and threaten access to Falls Creek. The compressed timeframe over which that understanding could be gained added to the challenge of understanding the geology, making the site safe and getting the road open.

2 EVIDENCE COLLECTED

The following evidence was collected to assist with the development of an engineering geological model of the Bogong landslide and to inform the basis of both the interim and permanent designs:

- Photographs and videos of the site, before, during and after the landslide event.
- Site observations collected by geotechnical engineers on site after the landslide event and during the initial clearance works.
- Geotechnical boreholes, including groundwater information.
- Publicly available geological and rainfall information.
- Surface survey information including both photogrammetry and LiDAR collected regularly using UAV techniques.
- Monitoring data, i.e. tilt sensors, collected continuously during clearance works.

Video and photographs taken in October 2022 on the day material reached the road indicate that material detached from the natural 40° slope upslope of benches 1 and 2. The debris travelled as a non-saturated soil (poured over like sand rather than flowed as a liquid) over the lower two benches. Based on the video and photos, slope materials did not detach from the lower two benches. However, materials may have been stripped from the benches as debris flowed over them. Seepage was not observed from the face, nor did it appear to be associated with the material detachment. Over the subsequent week further material detached from above Bench 2, causing debris to bury the lower benches and the buildup of a colluvial fan at the toe of the slope as indicated in Figure 2.

Comparison between LiDAR survey acquired before and after the landslide indicated a zone of soil depletion upslope of Bench 2 where material has detached and a zone of soil accumulation, where material has been deposited downslope of Bench 2. This is illustrated in the cross section in Figure 4. The location and geometry of the slip surface could be estimated through the survey comparison. Note that some material mobilised by the landlide was retained in the source area due to incomplete transportation to the zone of accumulation.

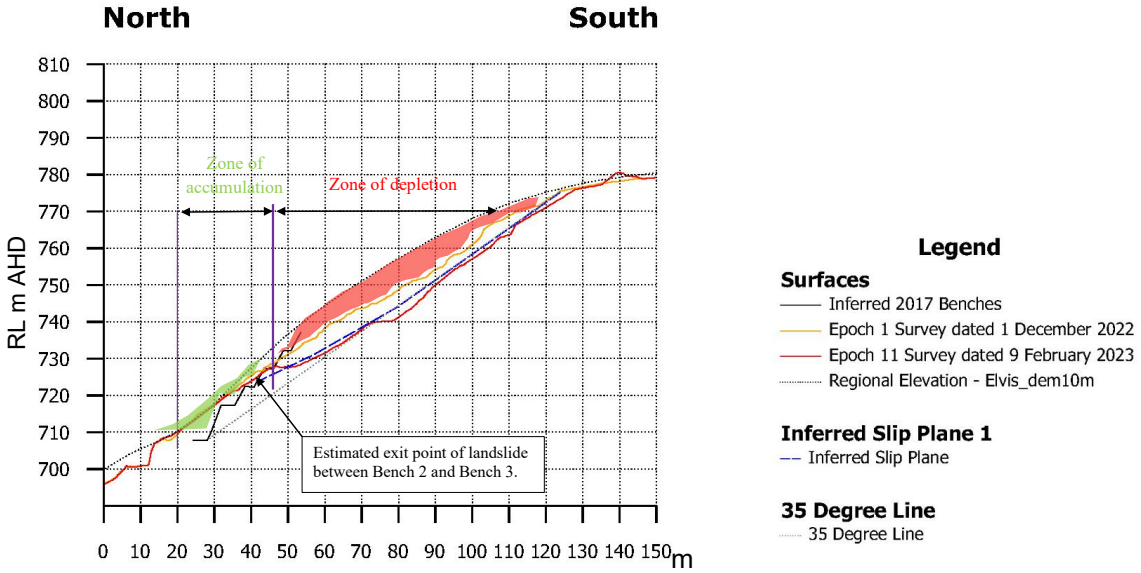

Figure 4: Indication of zones of accumulation and depletion associated with the October 2022 landslide

In early January 2023, debris clearance works sought to cut the slope bank to the landslide plane by removing the loose debris. Observations of the cleared surface indicate that the landslide plane was relatively shallow, with an angle of about 35° from the horizontal as indicated in Figure 5 and as confirmed by LiDAR and photogrammetry survey.

Figure 5: Crest of landslide, 12 January 2023 taken from Spring Saddle Track. Excavation has cut back to in situ material.

On 18 January 2023, in response to heavy rainfall (24 mm recorded at Falls Creek over the hours preceding the event), a crack opened within a batter slope about 10 m below the crest of the cutting made by the clearance works. Subsequent photogrammetry survey indicates the extent of the cracking and that it occurred on a slope of about 36° to 37° and regressed back to an angle of about 35°. Rills and gullies formed due to softening and erosion of the soils (Figure 8). Observations consistently indicated that where landsliding had occurred, it had occurred on sloping ground steeper than 35°, as measured from the horizontal and regressed back to 35°. This angle is consistent with the angle of repose for the debris at the base of the slope and suggested a friction angle within the soils of about 35° (Figure 6). The geomorphic evidence was consistent with triaxial evidence subsequently obtained.

Figure 6: Loose debris at toe of slope, 13 February 2023

Geotechnical investigations included drilling boreholes up to 40 m depth immediately upslope of the landslide headscarp and on its flanks. These boreholes did not encounter groundwater, indicating a deep groundwater table well below the landslide and suggesting that raising of the permanent groundwater table was unlikely to be a factor in the observed instability. Boreholes encountered unusually deep residual and extremely weathered micaceous granitic soils that appear to be associated with a sheared contact between two granite intrusions, consistent with geological map indications. The soils were typically partially saturated, although based on site observations, the moisture content of near surface materials respond rapidly to wetting and drying. Observations of earthworks indicated that steep batters can be cut when the material is in a partially saturated state. However, upon wetting or drying these steep batters collapse and regress. Measurements of loose, dry material in stockpiles indicated a consistent angle of repose for the material of 35°, an angle confirmed by LiDAR and photogrammetry survey.

3 POSTULATED LANDSLIDE MECHANISM

The apparent lack of free water or soil saturation associated with the landslide was a key indication that it was not triggered by the development of positive pore pressures within the slope, for example a rising groundwater table, which was confirmed through borehole groundwater measurements. Furthermore, the deep, fine-grained soils, lack of persistent structure (joints or other defects), the preceding above average rainfall and northerly aspect to the slope were assessed to be consistent with a landslide mechanism involving a loss of soil strength due to a loss of suction stresses. An engineering geological model was developed for the landslide based on a loss of suction stresses in the slope caused by increased moisture content.

In an unsaturated soil, suction stresses are induced by negative pore water pressures and strength is gained in the soil through apparent cohesion. Once the soil becomes saturated or the suction stresses are dissipated through a loss of soil structure, this gained strength or apparent cohesion is lost. Residual granitic soils exposed in slopes with a northerly or northwesterly aspect in Victoria have been recognized as prone to landslide upon saturation, Nyman (2013); Nyman et al., (2019). The relative difference between precipitation and evaporation on slopes with northerly or northwesterly aspect is greatest, which gives slopes of this aspect the potential to develop high soil suctions and suction stresses. Few landslides are observed in residual granites in Victoria during 'typical' climate conditions (neutral conditions between La Niña and El Niño events). However, based on the experience of the author's of this paper, soil wetting induced by prolonged or extreme rainfall in La Niña phases sees an increase in landslide and debris flow activity, particularly within granitic soils, which is what is inferred to have occurred at Bogong.

Similar landslide mechanisms in granitic soils been studied in locations such as Hong Kong, for example, Henscher and Lee, (2010). Figure 7 illustrates the concept of rainfall induced landslides caused by a loss of soil suction. As in this example, the 2022 Bogong landslide occurred in soils well above the water table that were not significantly influenced by positive pore water pressure. Note that no significant seepage or evidence of positive pore pressure development was observed to be associated with the Bogong landslide.

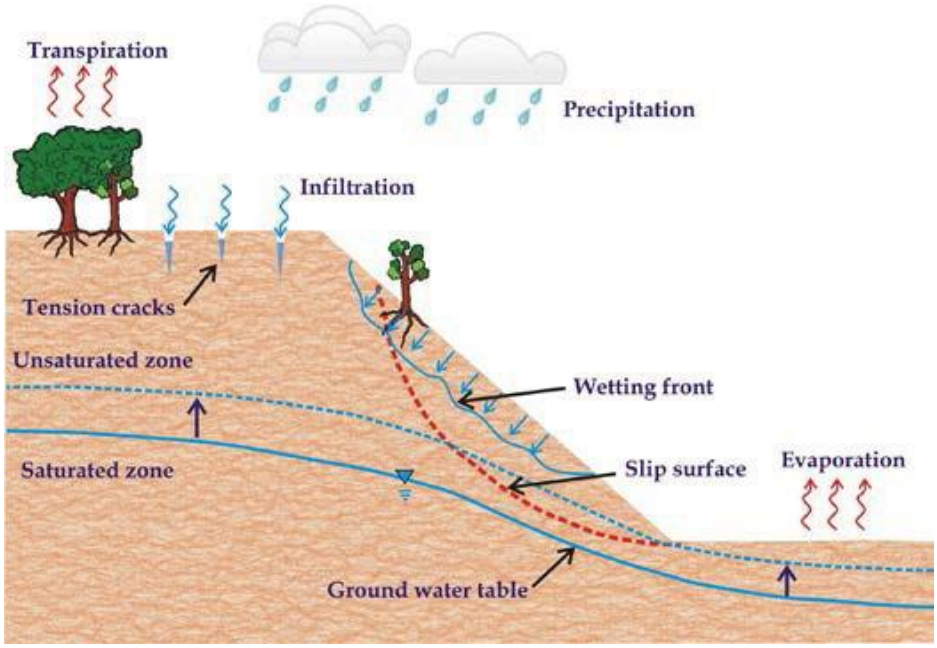

Figure 7: Concept for rainfall induced landslide in unsaturated soils, after Rahardjo et. al. (2011)

Strain in the form of tension cracks was first noticed upslope of the landslide, before there was any evidence of rupture in the face of the cutting at the toe of the landslide. It is postulated that the wetting front advanced into the slope commencing at the crest near what would become the headscarp of the landslide with the less saturated soils downslope. The tension cracks and some of the more permeable rocky strata within the slope may have been a conduit for water infiltration with the slope, effectively pushing displacement from upslope due to loss of strength in that area.

Whilst the loss of soil suction model for the landslide was consistent with observation, measuring the soil-water characteristics to help inform its geotechnical behaviour under unsaturated conditions takes a long time, with testing to derive a soil-moisture characteristic curve potentially taking months. Whilst this testing was ultimately done and used to help verify the model (see section 5), it occurred well after it was necessary to develop an interim design and get the road open. The project proceeded on the basis that the landslide mechanisms involved a loss of soil suction.

Observations and testing were undertaken to gather information on the basic geomechanical properties of the soils as follows:

- Classification testing, which indicated the material ranged span clayey sand, silty sand and sand. The proportion of fines ranged between 35% and 50% and were predominantly a low-plasticity silt. The materials are sufficiently fine grained to support high suction stresses, but permeable enough to be vulnerable to surface-water infiltration and loss of suction.
- The in situ bulk density ranged between 2.0 t/m^3 and 2.1 t/m^3, reducing to about 1.5 t/m^3 when disturbed and loose. These relatively low densities are consistent with the mica content and structured nature of the soils.
- Triaxial testing indicated an internal angle of friction consistently between 33° and 35°, consistent with the geomorphic evidence.
- Pinhole dispersion tests indicated the soils to be ‘erosion resistant’ whereas the Emerson class tests found the compacted material to be Class 5, moderately dispersive. This is consistent with the observations of gully erosion after heavy rains (Figure 8) and loss of trafficability, noting that rapid drying (within 24 hours) and return to trafficable conditions was observed.

Figure 8: Gully erosion after heavy rain, 18 January 2023

The interim design was advanced based on the assessment of soil properties set out above assuming a landslide mechanism involving a loss of soil suction.

4 BASIS OF REMEDIAL DESIGNS

Linked to the assessed landslide mechanism, the objectives of both the interim and permanent designs were to:

- Safely remove soil from and open the road, initially one lane for the interim remediation and two lanes for the permanent remediation.
- Reduce the risk to road users and residents of Bogong Village to a level tolerable by the road regulator.

- Preserve soil suctions insofar as is possible whilst also reducing reliance on suction stresses for stability.
- Given the location on the edge of Alpine National Park, preserve the natural landscape and ongoing maintenance requirements in the permanent solution by avoiding hard engineering measures wherever possible.

Estimation of the angle to which the slope should be cut back in both the interim and permanent case was undertaken using an infinite slope analysis adapted for unsaturated soil conditions after Lu and Godt (2009). This method was adopted because the sliding plane of the October 2022 landslide was roughly planar and persistent over a large area and because through approximation, this method allows consideration of suction stresses induced by unsaturated conditions without knowledge of the full soil-water characteristic curve (SWCC), noting this was not available within the short time frame over which remedial designs needed to be developed.

Lu and Godt (2008) provide a series of equations and examples for various soil types, including silty and sandy soil types similar to those underlying the site and which are prone to a loss of suction in response to wetting. These are based on the modification of a 'classic' infinite slope stability equation to consider the effects of apparent cohesion developed through soil suction stresses. This generalized infinite slope equation is noted for use in the assessment of stability within silty or sandy unsaturated soils above the water table where slope failure (factor of safety reduces below 1.0) is likely to occur in a weakened zone a few metres below the ground surface and furthermore, that failure occurs as the soil nears saturation and suction stresses approach 0.

Equation 1 is for stability analysis of unsaturated slopes as provided by Lu and Godt (2008):

$$F = \frac{\tan \emptyset\prime}{\tan \beta} + \frac{2c\prime}{\gamma H_{ss} \sin 2\beta} - \frac{\sigma^s}{\gamma H_{ss}} (\tan \beta + \cot \beta) \tan \emptyset' \quad (1)$$

Where:

- F is the factor of safety
- $\emptyset'$ is the effective friction angle in degrees (°)
- c' is the effective cohesion
- β is the slope angle in degrees (°) as measured from the horizontal
- H_{ss} is the depth to the sliding plane from the ground surface
- σ^s is the suction stress which is related to the volumetric water content
- γ is the soil unit weight

The first term in the equation relates to the internal friction or friction angle of the soils, the second to the cohesion and the third to the apparent cohesion or strength attributed to suction stresses. It was conservatively assumed there is no cohesion on the basis of the low plasticity and silty/sandy composition of the soils and based on observation that the soils are completely dry such that $\sigma^s = 0$, then a factor of safety, F of 1 is achieved when the slope angle approaches the friction angle. This is analogous to the angle of repose adopted by the landslide debris that accumulated at the toe of the slope and provides evidence in support of a friction angle of about 35° within the disturbed, loose residual soils.

LiDAR and photogrammetry survey indicated that the landslide had a depth to the sliding plane (H_{ss}) of up to about 7 m. Based on the Equation 1, and assuming no cohesion, a friction angle of 35°, a slope angle of 40° (indicated by survey and shown in Figure 4) and depth of 7 m to the failure plane, a factor of safety greater than 1 is maintained with as little as 0.25 kPa of soil suction. If the slope angle is reduced to 35°, the factor of safety with -1 kPa of suction stress is 2.0. Based on assessment using Equation 1, the effect of suction stresses on stability within these materials is significant and it is likely that prior to the landslide, the stability of the slope was dependent upon the preservation of suction stresses. Lu and Godt (2008) indicate a suction stress of -1 kPa can be achieved in unsaturated silty and fine sand materials with volumetric moisture contents as low as 10% and that with wetting, suction stress does not significantly reduce until the degree of saturation is above about 90%. Given the emergency nature of the works and in the absence of testing to assess the soil-moisture characteristics at the early stage of the project, these typical estimates were adopted to help confirm the postulated landslide mechanism. As set out in Section 5, field and laboratory testing was subsequently undertaken to test this hypothesis. The interim remedial design involved:

- Removing debris and cutting the slope back such that batter slopes were no steeper than 35°, estimated to be the maximum angle at which stability could be preserved (Factor of Safety greater than 1) if suction stresses were lost.
- Providing erosion control matting over the slope whilst in a temporary condition to reduce erosion and runoff.
- Opening of one lane of the road once the slope had been sufficiently cut back to uncover the lane in conjunction with monitoring and the implementation of a trigger/action/response plan (TARP).

The permanent design then involved:

- Providing 10 m wide benches to prevent debris reaching the road in the event there were to be instability on a batter slope. The overall slope angle was 27° and based on Equation 1 is estimated to have a factor of safety of about 1.4 under conditions where suction stresses are lost. The batter slopes themselves had a factor of safety approaching 1 under conditions where suction stresses were lost, necessitating the need to provide the benches to prevent landslides arising on the batters from reaching the road.
- Preserving the natural soil structure as far as practical. No fill was placed as part of the landslide remediation.
- Revegetating the slope using a mix of native vegetation to help preserve soil suctions.
- Proving bench drains to direct surface water off the landslide as efficiently as possible.
- Providing access tracks to help reduce surface water infiltration and to allow future slope maintenance such as clearing drains, removing debris and maintaining vegetative cover.

Images of the completed permanent works are shown in Figure 9 and Figure 10 and the designed permanent slope profile in Figure 11.

Figure 9: Far field view of remediated slope (bench 10 m wide)

Figure 10: View along completed bench (bench 10 m wide)

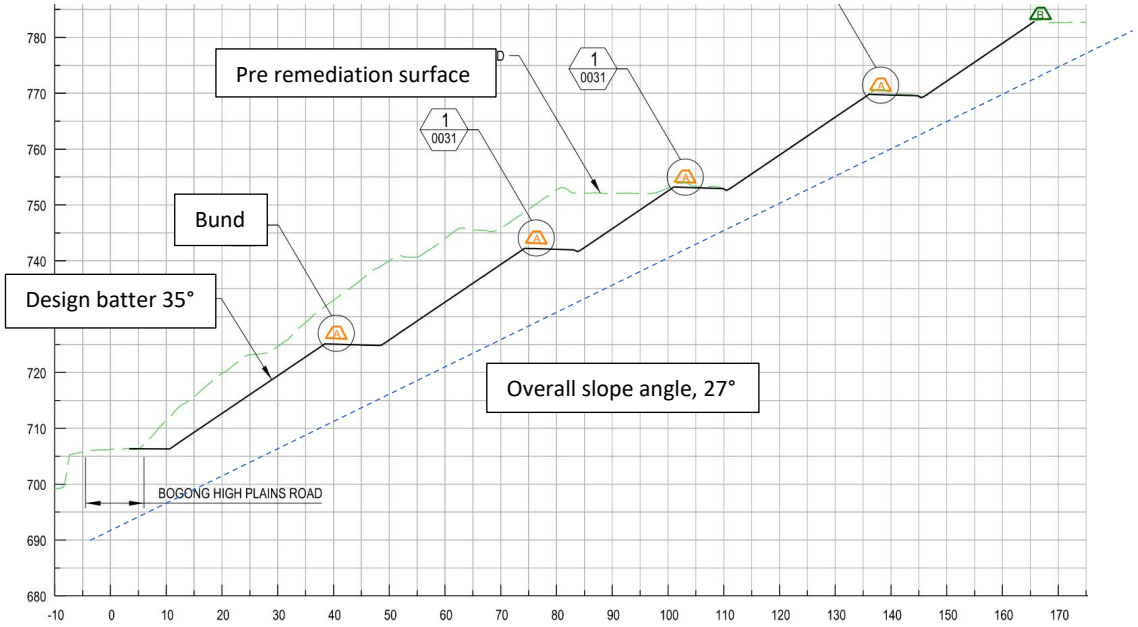

Figure 11: Typical cross section through remediated landslide (scale in m)

A risk assessment was undertaken to assess the risk to road users noting that achieving a risk level that could be tolerated by the road regulator was a requirement of the design. The key input to the risk assessment was the probability of a landslide, related in this case to the degree of saturation within the soils. Guidance was taken from literature to estimate the probability of failure for the slope within which the global factor of safety is expected to reduce to 1.4 every 50 years or so in response to wetting. Kavvadas et. al. (2009) presents a relationship between factor of safety and probability of failure for cohesive soils as indicated in Figure 12. On this diagram, V_{cu} is the coefficient of variation of c_u, (the undrained shear strength) and is a function of the certainty in that parameter calculated as the standard deviation divided by the mean for that parameter. The higher the coefficient of variation, the less certainty in the parameter and the higher the probability of failure. There was limited strength data on which to base an estimate of the coefficient of variation for the soils of the Bogong landslide. However, the observations that were undertaken, which included triaxial tests plus observations of the landslide, suggest a coefficient of variation of between 0.05 and 0.3 based on the measured friction angle and cohesion respectively. Whilst a highly uncertain estimate due to limited data, this is a low coefficient of variation, which is consistent with observations. Assuming a coefficient of variation of 0.25, a Factor of Safety of 1.4 correlates to a probability of failure of about 0.05.

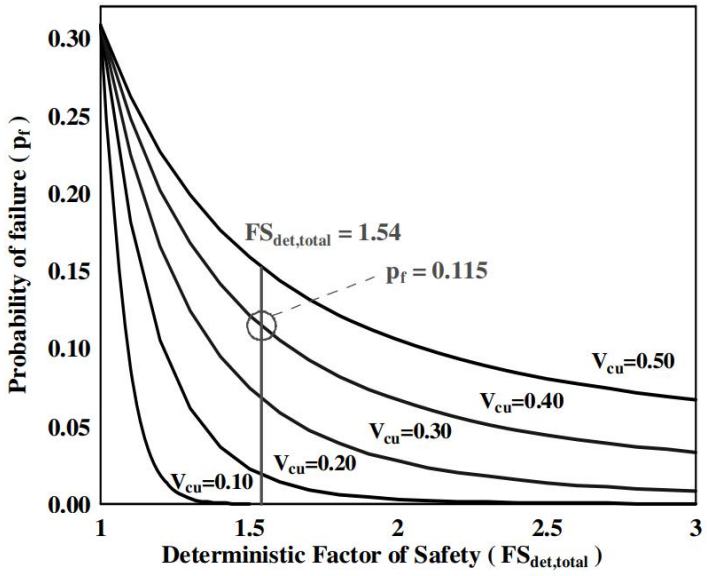

Figure 12: Extract from Kavvadas et.al. (2009) showing relationship between factor and safety and probability of failure for cohesive soil

This estimate is consistent with Read and Stacey (2009), who provide Table 1 indicating a general relationship between factor of safety and probability of failure and suggesting via interpolation a probability of failure of 5% (0.05) for a factor of safety of 1.4.

Table 1: General Relationship Between FOS and PoF, extract from Read and Stacey (2009)

Consequence of failure impacting on public safety, infrastructure, environment, land or property	Acceptable (mean) FOS	Acceptable minimum PoF
Not Serious	1.3	10%
Moderately Serious	1.6	1%
Very Serious	2.0	0.5%

Based on these indications, albeit it relatively uncertain, a probability of failure of 0.05 was assumed for global instability of the four-bench design. Assuming the probability of the slope becoming saturated is about 1 in 50 (0.02) and the probability of failure under that condition is 0.05, the probability of global failure was estimated as the product of 0.02 × 0.05 = 0.001 or 1 in 1,000. This corresponds to an 'Unlikely' probability and 'Medium' risk assuming the consequences of another similar landslide would be 'Major' when assessed using the risk matrix as shown in Figure 13 after the road regulator. This assessed risk level was sufficient to satisfy the road regulator and the road was permanently reopened back to two lanes on that basis.

Table 1: Risk estimation matrix for road geotechnical hazards.

Likelihood	Consequences				
	1 or C1 CATASTROPHIC	2 or C2 MAJOR	3 or C3 MEDIUM	4 or C4 MINOR	5 or C5 INSIGNIFICANT
A or L1 ALMOST CERTAIN	VH	VH	H	H	M
B or L2 LIKELY	VH	H	H	M	L-M
C or L3 POSSIBLE	H	M-H	M	L-M	VL-L
D or L4 UNLIKELY	M-H	M	L-M	L	VL
E or L5 RARE	M	L-M	L	VL	VL
F or L6 NOT CREDIBLE	VL	VL	VL	VL	VL

Estimated based on bulk earthworks

Target

Figure 13: Extract from VicRoads Technical Note TN-96 (Vicroads, 2022)

5 VERIFICATION OF LANSDLIDE MECHANISM

To further investigate the postulated landslide mechanism, in-situ soil moisture and soil suction sensors were installed and laboratory testing undertaken to establish a SWCC. Four soil moisture sensors and two soil suction sensors were installed between 0.5 m and 1 m depth in clayey sand material (residual granitic soil to extremely weathered granite). Sensors were installed in three auger holes (two sensors per auger hole) in remediated benches 1, 3 and 4. Auger holes were excavated using a hand auger with the moisture sensors embedded in the hole sidewalls (in-situ soil) and suction sensors placed in compacted backfill at the base of the hole. Holes were backfilled by hand with spoil at approximately 100 mm increments and tamped by hand. Laboratory testing was undertaken on a single undisturbed tube sample taken from bench 3 in similar clayey sand material (residual granitic soil).

A SWC-150 pressure plate device was used to measure volumetric water contents for matrix suction values on the drying and wetting curve of less than 1000 kPa. A WP4C water potential meter was used to measure water contents for matrix suction values on the drying curve above 1000 kPa. Figure 14 shows the SWCC developed. Testing covered suction stages ranging from 9 kPa to 316 kPa on the wetting curve and between 77 kPa and 147 MPa on the drying curve. These corresponded to a variation in volumetric water content of between 18.9% and 46.9% on the wetting curve and 3.9% and 26% on the drying curve.

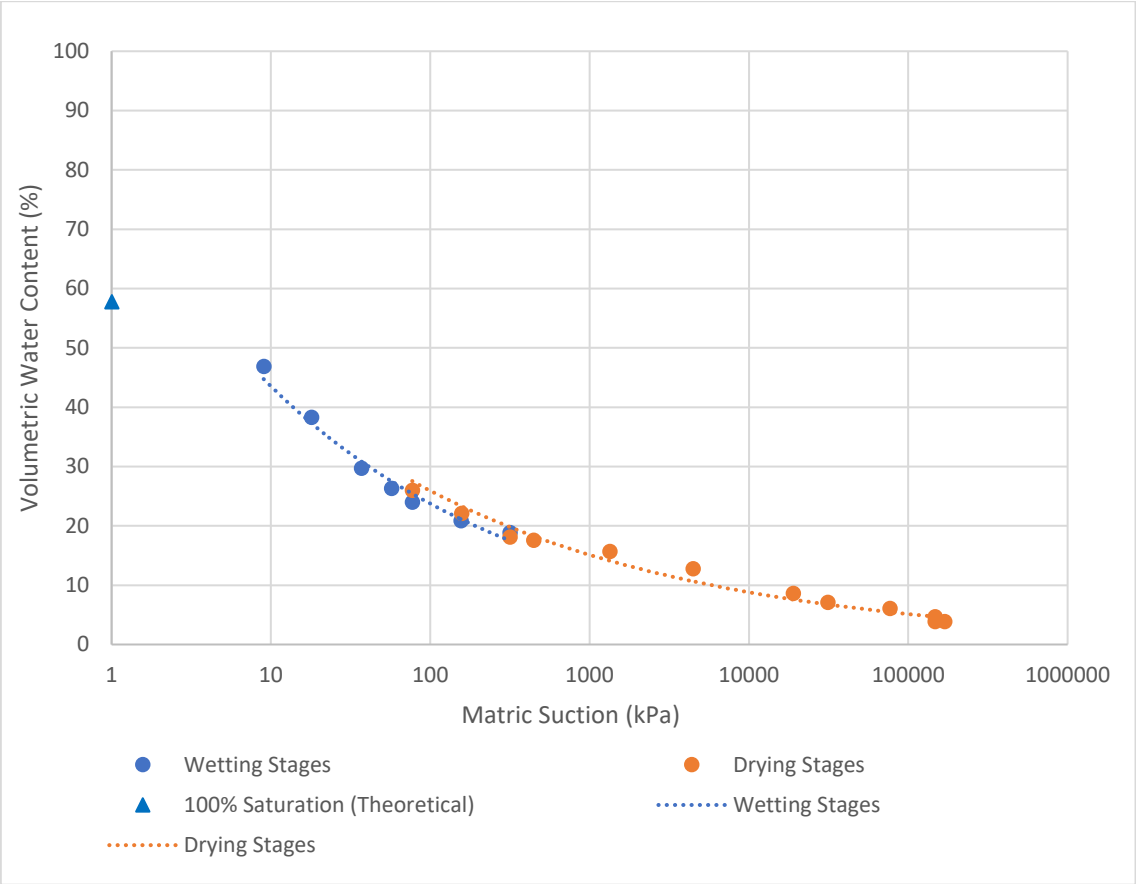

Figure 14: Soil water characteristic curve

The relationship measured between volumetric soil moisture and rainfall over a six-month period is presented in Figure 15. More than six-months of in-situ soil moisture data indicated a strong relationship between rain events and soil moisture, generally a sharp increase in soil moisture in all four sensors in response to a rain event followed by a gradual decrease in soil moisture. Smaller, but more frequent, rainfall events during September appear to correspond to a higher average soil moisture.

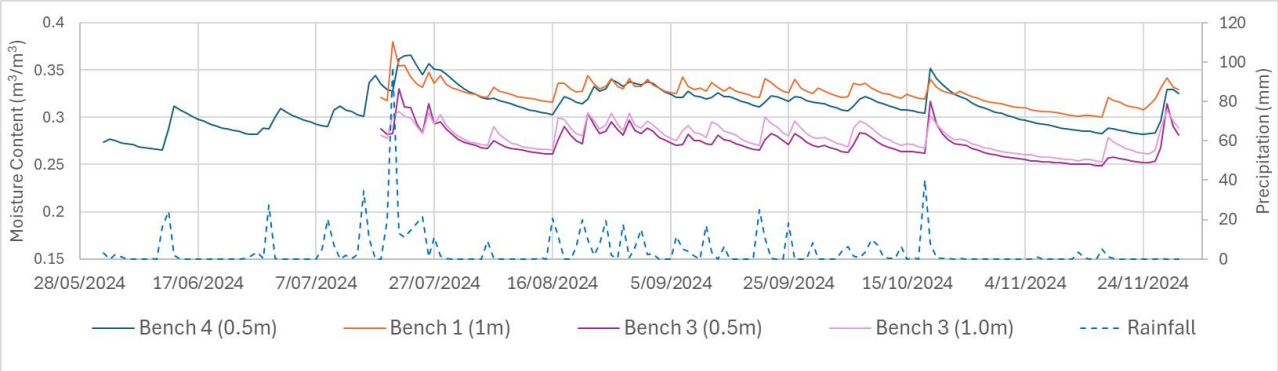

Figure 15: Measured relationship between rainfall and soil suction

The SWCC developed in Figure 14 was used to convert the in-situ volumetric soil moisture measurements into a matric soil suction. Site-measured soil moisture was between 25% and 40%, which fell between laboratory measured moisture conditions, i.e. not outside the range of available data points used to generate the SWCC. Rainfall together with the measured soil suction and corresponding soil suction developed from the measured soil moisture and SWCC is plotted in Figure 16.

The measured soil suction generally followed a similar, but inverse, pattern as the soil moisture with sharp decreases in soil suction measured following rain events followed by a gradual increase in periods of no rainfall. During winter and spring months (July to October) several instances of zero suction occurred, likely due to frequent rainfall events during this period. Compared to the measured soil suctions, the soil suctions estimated by SWCC were significantly higher, showed more variation and did not show instances of zero suction.

These differences could be due to the SWCC better estimating soil matric suction for in-situ soil compared to the disturbed soil at the base of the borehole in which the sensor was installed. Another potential cause for differences could be the differences in soil composition tested in the laboratory compared to the soil the sensors were installed in.

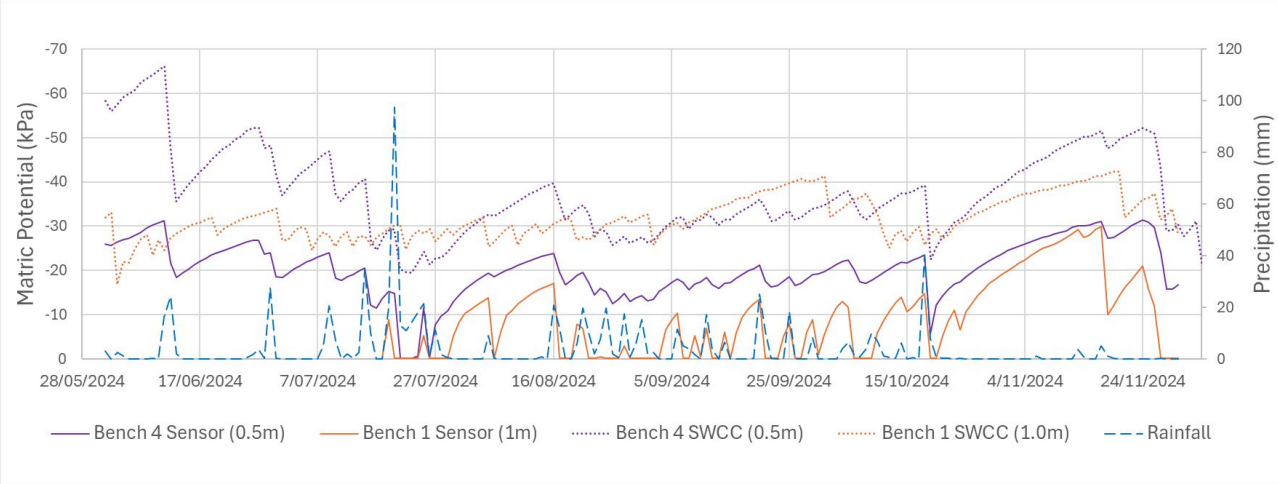

Figure 16: Relationship between rainfall, and estimated matric suction and estimated matrix suction from SWCC

The soil moisture and suction data presented in Figure 15 and Figure 16 indicate two important behaviours of the residual granitic soil consistent with the postulated landslide mechanism:

- The soil suctions are sensitive to rainfall and show seasonal change with frequent rainfall events causing a loss of suction.
- Disturbed soil appears to hold significantly less suction as implied by the differences in SWCC estimated suction and measured suctions from the sensors installed in backfilled material.

Measured soil suctions ranged between 0 kPa and -31 kPa, whereas estimated soil suctions ranged between -16 kPa and -66 kPa. This significant change in effective cohesion support the model that that the Bogong landslide could have occurred due to a general increase in soil moisture during a period of increased rainfall leading to a reduced overall matric soil suction in the slope. Furthermore, if disturbance of the in-situ soil occurred due to failure of the soil matrix, it is likely a significant amount of suction (and therefore effective cohesion) would have been lost near the zone of failure.

6 CONCLUSIONS

Understanding the landslide mechanism was crucial to the selection and design of remedial works for the Bogong landslide. Given the emergency nature of the event, that understanding had to be developed using the best evidence available at the time. Deep residual granites combined with a northerly slope aspect and the apparent lack of free water in the landslide were suggestive of a landslide mechanism involving a loss of soil suction stresses induced over a period with prolonged, above average rainfall.

Remedial solutions were developed in line with this postulated mechanism and involved cutting the slope back to an angle such that reliance on suction stresses for stability was reduced along with works to preserve suction stresses, including drainage and revegetation.

Based on the studies undertaken into the Bogong landslide, landslide mechanisms in southern Australia involving a loss of soil suction is an area for further study. It is postulated that slopes in southern Australia with a northerly aspect are more susceptible to this type of landslide mechanism because they have the greatest differential between precipitation and evapotranspiration. Deeply weathered soil profiles, such as those typical of granitic rocks, can maintain oversteep angles, including in human-made slopes such as road cuttings due to their partial saturation. Approaches to landslide mitigation measures that focus on the preservation of soil suctions in lieu of hard engineering measures should be pursued.

7 REFERENCES

Kavvadas, M., Karlaftis, M., Fortsakis, P., Stylianidi, E. (2009) Probabilistic analysis in slope stability, *Proceedings of the 17th International Conference on Soil Mechanics and Geotechnical Engineering,* pp1650 – 1653.

Lu, N., Godt, J. (2008), Infinite slope stability under steady unsaturated seepage conditions, water resources research, Vol 44 (11) W11404.

Henscher, S.R., Lee, S.G. (2010) Landslide mechanisms in Hong Kong, in *Weathering as pre-disposing factor to slope movements, Geological Society of London, Special Publication 23*. pp 77 – 103.

Nyman. P. (2013) Post-fire debris flows in southeast Australia: initiation, magnitude and landscape controls, PhD thesis, University of Melbourne.

Nyman, P, Rutherford, I.D., Lane, P.N.J., Sheridan, J.,(2019) Debris flows in southeast Australia linked to drought, wildfire and the El Nino-southern oscillation, *Journal of the Geological Society of America*, 47 (5).

Rahardjo, H., Satayanaga, A., Leong, E.C. (2011) Unsaturated soil mechanics for slope stabilisation, *Unsaturated soils: theory and practice, Jotisankasa, Sawangsuriya, Soralump and Mairaing (ed.),* Kasetsart University, Thailand. Pp.103-117

Read, J., Stacey, P., (2009) Guidelines for Open Pit Slope Design, *CSIRO Publishing*

VicRoads. (2022) Technical Note TN096, Version 3, available from https://content.vic.gov.au/sites/default/files/2024-05/Technical-Note-TN-096-Risk-Management-of-Road-Geotechnical-Hazards.pdf.